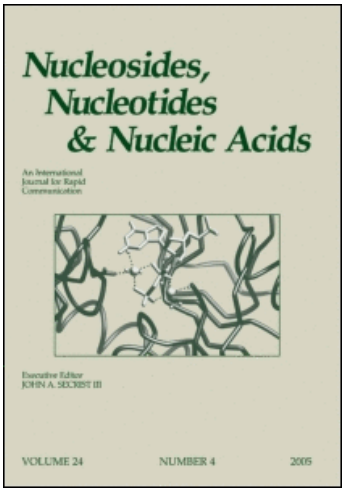

Nucleosides, Nucleotides and Nucleic Acids
Publication details, including instructions for authors and subscription information:
http://www.informaworld.com/smpp/title~content=t713597286

The Parallel and Antiparallel Triplex Formation and Stability of Self Complementary Oligonucleotides Containing 2'-Fluoro-arabinosyl Thymine and 5-Methyl-2'-Deoxycytidine

Wu. Yun Ren[a]; Kyoichi A. Watanabe[a]
[a] Codon Pharmaceuticals, Inc, Gaithersberg, MD

To cite this Article Ren, Wu. Yun and Watanabe, Kyoichi A.(1998) 'The Parallel and Antiparallel Triplex Formation and Stability of Self Complementary Oligonucleotides Containing 2'-Fluoro-arabinosyl Thymine and 5-Methyl-2'-Deoxycytidine', Nucleosides, Nucleotides and Nucleic Acids, 17: 9, 2103 — 2116
To link to this Article: DOI: 10.1080/07328319808004753
URL: http://dx.doi.org/10.1080/07328319808004753

NUCLEOSIDES & NUCLEOTIDES, 17(9-11), 2103-2116 (1998)

THE PARALLEL AND ANTIPARALLEL TRIPLEX FORMATION AND STABILITY OF SELF COMPLEMENTARY OLIGONUCLEOTIDES CONTAINING 2'-FLUORO-ARABINOSYL THYMINE AND 5-METHYL-2'-DEOXYCYTIDINE

Wu Yun Ren and Kyoichi A. Watanabe

Codon Pharmaceuticals, Inc., 200 Perry Parkway, Gaithersberg, MD 20877

ABSTRACT: We examined the effects of 1-(2-deoxy -2-fluoro-β-D-arabinofuranosyl)-thymine (or FMAU, a potent antiviral nucleoside) on the stability of duplex and triplexes. When compared the stability of the self-complementary 5'-A_5T_5 duplex with 5'-A_5X_5 (X = FMAU), duplex containing FMAU has much higher melting temperature (T_m). 5'-$A_6T_5T_3X_3T_5F_3X_3$ and $T_3X_3T_5A_6T_5F_3X_3$ form the parallel and antiparallel triplexes T_3X_3:A_6:X_3T_3, respectively. The former exhibited the typical T:A:T triplex behavior with only one melting temperature at 70 °C and 45 °C in 1.0 M and 0.2 M NaCl solution, respectively, whereas the latter has two T_m values at 56 °C and 28 °C in 1.0 M solution. FMAU clearly stabilize the triplex structure as A_6T_{22} which forms the parallel triplex T_6:A_6:T_6 has also only one T_m at 54 °C and 37 °C in high and low salt concentration solutions, respectively. A 31mer 5'-TCCTCCTTTTTTAGGAGGATTTTTTGGTGGT and 5'-TCCTCCTTTTTTAGGAGGATTTTTTX'X'TX'X'T (X' = 2'-deoxy-5-methyl-cytidine) were prepared to study their triplex forming potential. The former was found to have a week interaction of the Watson-Crick duplex with the mismatched third-strand at all pH. The latter formed a stable triplex at lower pH consistent with required protonation on the 5-methylcytosine base. For these studies we developed a simple PC desktop spreadsheet program to calculate the first derivative profile of the melting curve data.

INTRODUCTION

We have been interested in the effects of biologically active nucleosides, which we synthesized, on the stability of double[1-4] and triple[5] helices of oligodeoxynucleotides. Since 1957 when the first triple helical polynucleotide complexes were reported by Felsenfeld *et al.*,[6] a variety of triple helices were subsequently observed.[7-10] Triple helical structures of DNA can be divided into two distinct structural classes: pyr:pur:pyr and

This paper is dedicated to Prof. Jacques H. van Boom on the occasion of his 60th birthday.

pyr:pur:pur motifs. The third strand binds to the Watson-Crick base pairs of the DNA double helix in the major groove. A double helix is a composite of two antiparallel strands. In a pyr:pur:pyr type triple helix, the third pyrimidine chain is bound to the double helix through Hoogsteen hydrogen bonding in a parallel fashion[11] with respect to the purine strand whereas in the pyr: pur:pur motif, the third purine chain is bound antiparallel to the middle purine strand through reverse Hoogsteen fashion.[12-15] The conformations of DNA triplexes containing isosteric 1-(2-deoxy-2-fluoro-ß-D-arabino-furanosyl)thymine (2'-F-5-Me-ara-U or FMAU) (**FIGURE I**) is of considerable interest because of its potent antiviral[16-18] and anticancer[19,20] properties. It is well documented that FMAU[2,3] enhances binding affinity and 5-methyl-2'-deoxycytidine (5-Me-CdR) permissive pH range in a double helix formation.[21] We used FMAU and 5-Me-CdR for our studies. It was mentioned that the stability of a triple helix is influenced by the length of oligonucleotide, base sequence, salt concentration, pH and modification of base, sugar and phosphodiester backbone based on experimental data.[22] To eliminate a potential equal concentration problem during the double or triple helix formation, we designed sequences **1** - **8** (**FIGURE II**) in which we linked three short oligonucleotides with two half turn 5-T loop structures.[23] This also fixed the orientation of the third strand. As we expected oligomers **3** - **7** formed their corresponding self folding complementary triple helical structure in solution. The decamers $d(A)_5(F)_5$ (**2**, F= FMAU) and $d(A)_5(T)_5$ (**1**) were prepared as our counterpart double helical references and the 28mer **3** which contain only natural nucleoside bases as our triple helical reference. The hair pin structure **8** is a 19mer which has a sequence of 5'-TCC TCC TTT TTT AGG AGG A. Sequences **4** and **5** have a T:A:T mode, but half of the thymidines are replaced by FMAU (**FIGURE I**). The 28mer **4** has a sequence of 5'-AAA AAA TTT TTT TTF FFT TTT TFF FTT T . Sequence **4** has the Pyr:Pur:Pyr motif in which the third strand is parallel to the purine sequence. In order to construct a sequence which has a similar double helical structure as sequence **4** but has an antiparallel third strand orientation to the purine chain, we designed sequence **5** (5'-TTT FFF TTT TTA AAA AAT TTT TFF FTT T). Sequences **6** 5'-TCC TCC TTT TTT AGG AGG ATT TTT TGG TGG T has a pyr:pur:pyr and pyr:pur:pur mix which would make the third strand to be an antiparallel arrangement to the second strand. Sequence **7** has a pyr:pur:pyr motif with an antiparallel third strand in which 5-Me-CdR was used instead of deoxycytidine (**FIGURE I**).

The thermal melting measurement is the primary tool for our search for the stability of double or triple helical structure of oligonucleotides. The transition from a helical structure to an unstacked, strand-separated coil is dependent on the temperature and concentration of inorganic salts. The temperature *vs.* absorbance graphs were plotted to

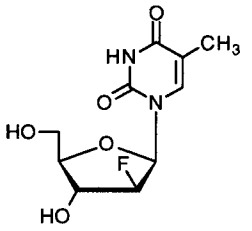

FMAU

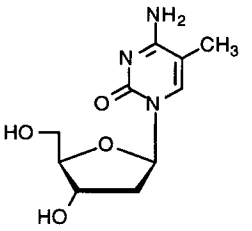

5-MeCdR

FIGURE I

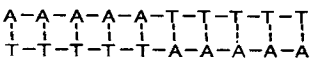

1

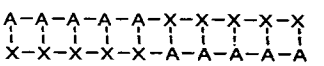

2

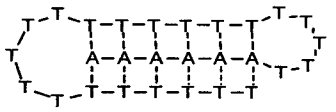

3

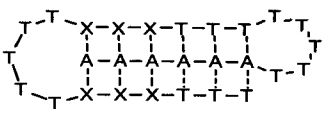

4

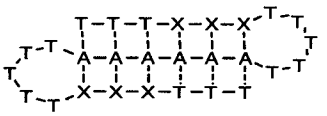

5

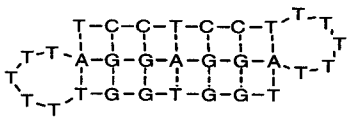

6

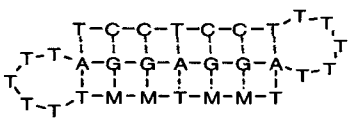

7

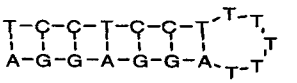

8

FIGURE II

give thermal denaturation (melting) profiles from which melting temperatures (T_m values) were determined. Besides T_m, the melting-curve profile provides important information about the state of dissociation of double or triple helix.

During the course of T_m measurements of triplexes, we encountered that the slope of the melting line was frequently of small amplitude which made it difficult to determine T_m accurately. To extract T_m information from such profiles, we decided to apply the first derivative of the curve. Theoretically, the first derivative of melting curves will take the

shape of Gaussian distribution and should provide more accurate results than the original melting temperature curves. The resulting line is dependent only on the slope increment or decrement; it is independent of concentration. This method gives us an advantage and convenience in determining T_m and in comparing different data sets.

In this report, we present the effects of FMAU and 5-MeCdR on the stability of duplex and triplex formation by analyzing thermal denaturation behavior of our model oligonucleotides. A simple and convenient spreadsheet program for the first derivative calculation was also developed.

METHODS

We synthesized all oligonucleotides **1** - **8** by the phosphoramidite method[24-26] in our modified GeneSyn I synthesizer[1]. 5-Me-CdR was prepared from thymidine.[27] Preparation of the phosphoramidite derivative of 5-Me-CdR was achieved by protecting the amino group with benzoic anhydride in refluxing ethanol and then protecting the 5'-hydroxy with dimethoxytrityl chloride followed by phosphitylation with 2-cyanoethyl N,N-diisopropylchlorophosphoramidite. In a similar manner we also prepared the 2-cyanoethyl N,N-diisopropylphosphoramidite derivative of FMAU. Using a longer coupling time and normal cycle, we found that 2'-fluoro nucleoside acted like a ribo-nucleoside, which gave an unacceptable yield due to the presence of an electronegative fluorine substituent. In an alternative approach, we activated the phosphoramidite agent by phosphitylation with methyl N,N-diisopropyl phosphoramidite instead of 2-cyanoethyl N,N-diisopropylphosphoramidite. The product of this approach allowed us to use FMAU just like a regular thymidine for routine synthesis of any sequence in an automatic synthesizer. All oligonucleotides were synthesized in an automatic DNA synthesizer. The DMTr group of the 3'-end was kept intact. After cleavage from the solid support and deblocking with 40% NH_4OH, the oligonucleotides were purified by HPLC on a C18 reversed phase column eluted with a 40 minutes 0 to 100% linear gradient of 70% aqueous acetonitrile (solvent B) in 0.1 M triethylammonium bicarbonate (solvent A). The gradient was 0% to 100% B in 40 minutes. The 5'-DMTr of the 5'-end was deprotected with 80% acetic acid. The pure product was obtained by a second HPLC purification and desalted with Sephadex G-25 column followed by AG50-8X ion exchange column to insure no contamination of triethylamine.

Melting temperatures of the oligomers were measured on a Gilford response II UV/VIS spectrophotometer with an automatic temperature control device. The absorbance was measured at UV_{max} = 260 nm with temperature range from 0 °C to 90 °C at 0.1 or 0.5

degree increments. The oligonucleotide was dissolved in 0.2 or 1M NaCl solution for measurement and the pH adjusted with a phosphate buffer. The data were collected and analyzed by using a program that we developed.[28] The program developed had two functions in our studies: tailoring the data set for further analyses and drawing the smooth first derivative curve. To smooth the curve the whole data set was treated as a combination of small linear fragments. Every minute fragmental straight line was joined head to tail to the next fragment to form a complete curve. Each fragment was calculated by linear regression to give the slope and the intercept of the line. In this calculation five data points were used for regression statistics values and each segment overlapped four data points. The first data point of the new segment was the second trend point of the last calculated value. We used three steps in our calculations. In the first step, one macro call was used \h to group every five data points to give an average value.[29] In the second step, macro \b was used to automatically eliminate all blank lines between the new data set.[30] The third macro named \a performed the first derivative calculations for our graphic comparison studies.[31] It first started to input the first five temperatures and data cells as independent and dependent blocks to use as a built-in regression function to perform the regression calculation and change the first data value to calculate the value and copy the *x coefficient* value as the primary first derivative value. The whole operation moved down one cell each time to perform regression for five cell blocks to give an overlapping average first derivative result for the whole spectrum. This simple method gave very satisfactory results.

RESULTS AND DISCUSSION

The self complementary double helix **1** has Tm at 13 °C (1M NaCl) and < 5 °C(0.2M NaCl) (Figure **3**). Its counterpart FMAU oligomer **2** has T_m at 25 °C (1 M NaCl) and 21 °C (0.2 M NaCl) (**FIGURE III**). The ΔT_m close to 10 °C between **1** and **2** in high salt concentration solution and ΔT_m is even larger in a low salt solution. These results clearly show the $d(A)_5d(F)_5$ (**2**) formed a much more stable helix than $d(A)_5d(T)_5$ (**1**). The hair pin type oligonucleotide **8,** due to their stronger C:G pair, has T_m at 70 °C (1M NaCl) and 62 °C (0.2 M NaCl) (**FIGURE VII**). The parallel self complementary pyr:pur:pyr triplex **3** and **4** gave a sharp typical melting curve with T_m at 45 °C in 0.2 M NaCl and 70 °C in 1 M NaCl solution for **4** and T_m at 37 °C in 0.2M NaCl and 54 °C in 1M NaCl for **3**, respectively (**FIGURE IV**). Sequences **5**, **6** and **7** all show a slow climbing melting

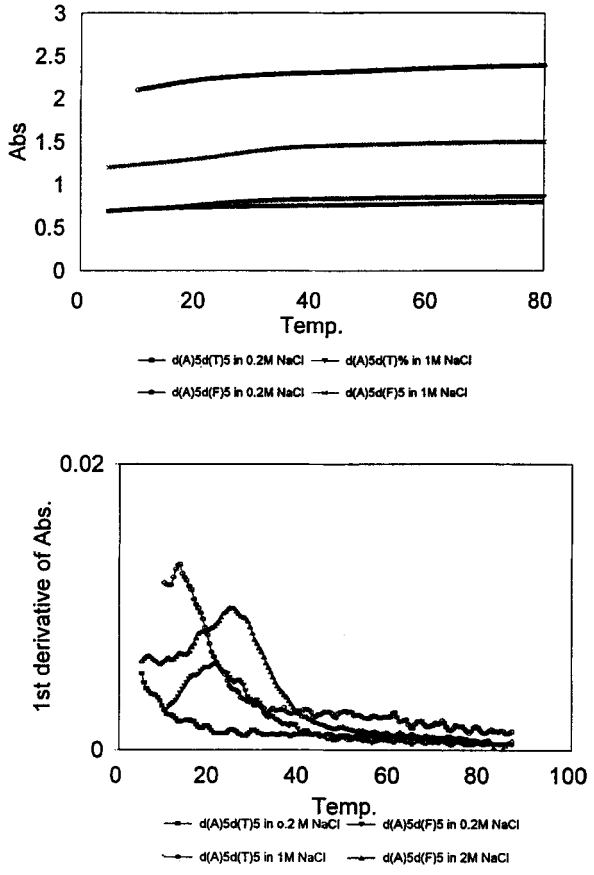

FIGURE III. The self complementary double helix **1** had T_m at 13°C (1M NaCl) and <5°C(0.2M NaCl). Its counterpart FMAU oligomer **2** had T_m at 25°C(1M NaCl) and 21°C(0.2M NaCl)

curve at a temperature range from 50 °C to 90 °C (**FIGURES V, VII** and **VI** for **5**, **6** and **7**, respectively). Sequence **5** also has an observed additional rise and slightly higher bump on the way up at 1 M NaCl solution. In general, curves for sequences **5**, **6** and **7** are not as sharp as those **1** ,**2** ,**3, 4** and **8**. After the T_m data were imported to the Quattro Pro spreadsheet program in the PC computer for the first derivative calculation, sequences **1, 2** ,**3, 4** and **8** displayed a single Gaussian lineshape curve in their first derivatives of absorbance *vs* temperature change (the lower part of **FIGURE III** for **1** and **2**, **FIGURES IV** and **VII** for **4** and **8,** respectively). The maximum reading temperature values correspond to the mid-point of original curves. The first derivative of sequences **5,**

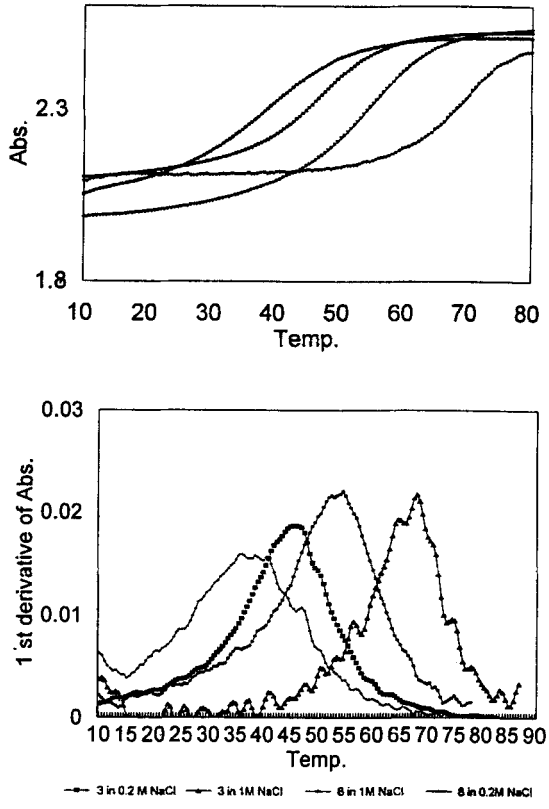

FIGURE IV. The parallel self complementary pyrimidine motif triplex **3** and **4** gave a sharp typical melting curve with T_m at 45°C(0,2M NaCl) and 70°C(1M NaCl) for **3** and Tm at 37°C(0.2M NaCl) and 54°C(1M NaCl) for **4** respectively.

which had an antiparallel pyrimidine third strand in the pyr:pur:pyr motif, gave a distinguished twin peaks maxima at 28 °C and 56 °C in 1M NaCl solution. Both peaks shifted to lower temperature regions in 0.2 M NaCl solution (**FIGURE V**). Under similar conditions, its counter-part corresponding parallel sequence **4** only showed one T_m at 45 °C in 0.2 M NaCl solution and 70 °C in 1 M NaCl solution (**FIGURE IV**). We also noticed that sequence **7** gave a double unsymmetrical Gaussian curve with maxima at 28 °C and 75 °C in 1M NaCl and pH = 6.0 buffer solution (**FIGURE VI**), respectively, and sequence **6** displayed only one unsymmetrical maximum. We measured the melting temperature of sequences **5**, **6** and **7** in pH = 6.0, 6.5, 7.0, 7.5. Sequence **6** did not show

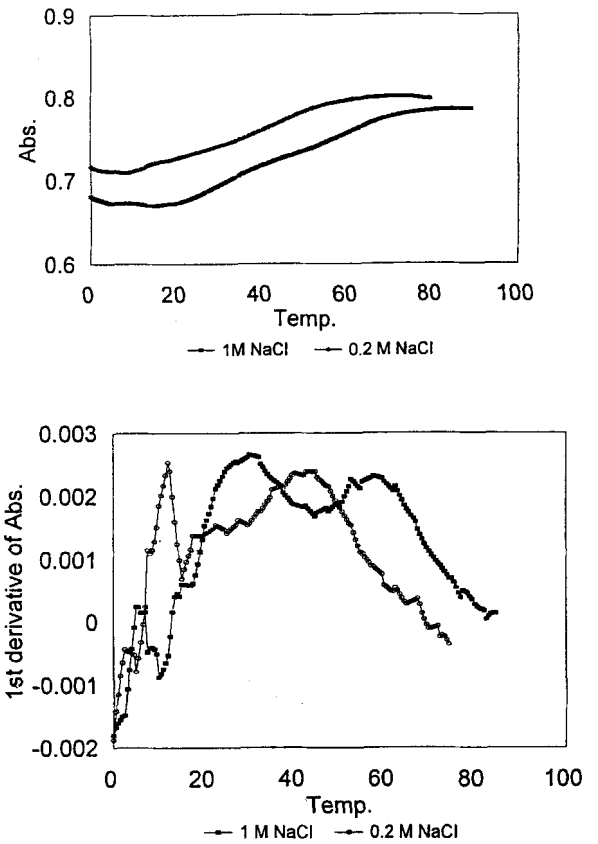

FIGURE V. The antiparallel motif sequence **5** gave a distinguished twin peaks maxima at 28°C and 56°C in 1M NaCl solution. Both peaks shifted to lower temperature regions in 0.2M NaCl solution.

any distinguishable structural change in all pH ranges. Sequence **7** gave reasonable triple helical interaction at pH = 6.0 (**FIGURE VI**) and this result is consistent with the reported observation which stated that 5-Me-CdR enhanced the triplex binding affinity. The sequence **5** displayed an identical result in all pH range which clearly indicated that the triple helical interaction of **5** was consistent and pH independent. The most interesting sequences were **3** , **4** and **5** which presented very unique T_m in both parallel and antiparallel orientation. The sequence **5** presumably formed an antiparallel pyr:pur:pyr conformation. An antiparallel mode of pyr:pur:pyr triplex would break the third pyrimidine chain to form any reasonable H-bonds between N7 and C6-NH_2 of adenine of the second strand and O4 and N3-H of the pyrimidine of the third strand as reported.[32] However, the

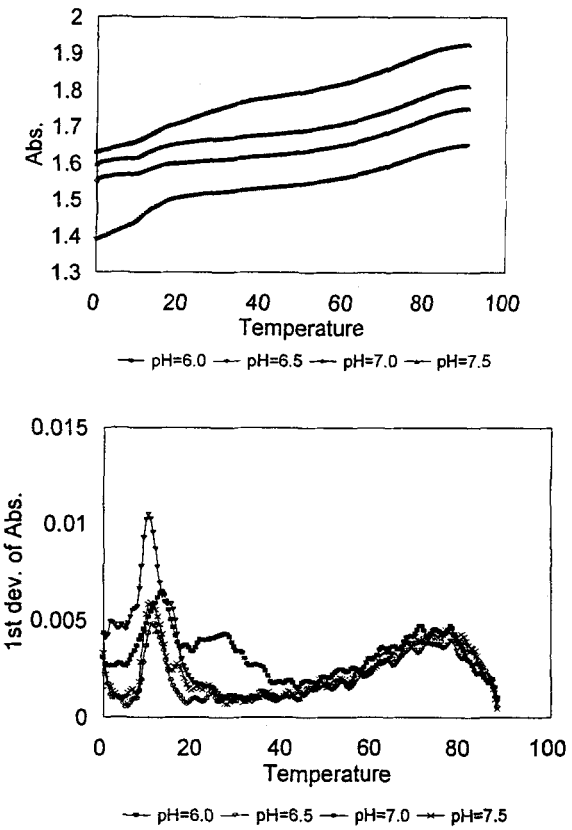

FIGURE VI. The sequences **7** had a mixed pyrimidine motif gave an undistinguishable triple helix with T_m at 75°C and shaw the second maximum at pH=6.0

first derivative of the melting curve of **5** clearly exhibited two stages of interaction in our experimental result (**FIGURE V**). *This strongly suggests that even antiparallel T:A:T conformation can form weak triple helical structures under certain conditions.* Thus, the higher T_m (56 °C) of **5** in 1M NaCl represented the double helix dissociation temperature and lower T_m (28 °C) represented the dissociation temperature of the third strand. The parallel triplex **3** and **4** have only one T_m at 70 °C and 54 °C in 1N NaCl solution and 45 °C and 37 °C in 0.2N NaCl solution respectively and which is ten degrees higher than the double helical dissociation temperature of the counterpart structure **5** and sixteen degree higher than the natural base sequence **3** in the case of 1N NaCl solution. This one melting temperature for triplex structures of **3** and **4** may explain that the Hoogsteen base pair and

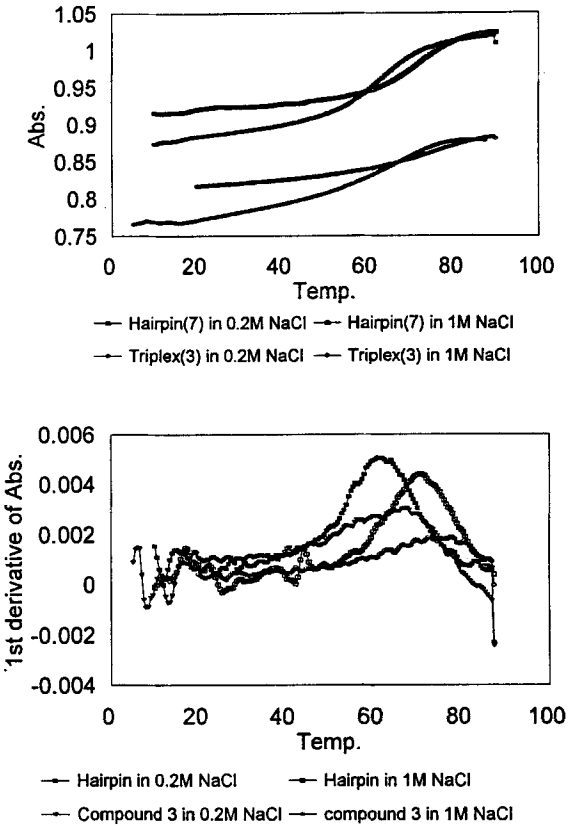

FIGURE VII. The hair pin **8** gave a sharp T_m at 70°C(1M NaCl) and 62°C(0.2M NaCl). The sequence **6** with a mixed of pyrimidine and purine motif gave almost no T_m.

the Watson-Crick base pair have equal strength in this case. The stacking force of the triple helix actually fused the three DNA chains together to form an equally strong and associated strand as some modeling studies reported.[33]

CONCLUSION

Our study suggests that when a double helix comes in contact with another oligonucleotide, even though they may not form a true, perfect triplex, they will still have a mutual interaction. It appears that the geometry fitness is the key to forming strong triple helices and the matching base pairs is essential for the third strand. The highly recognized parallel T:A:T triplex **3** and **4** gave only one melting temperature, fully reflecting its

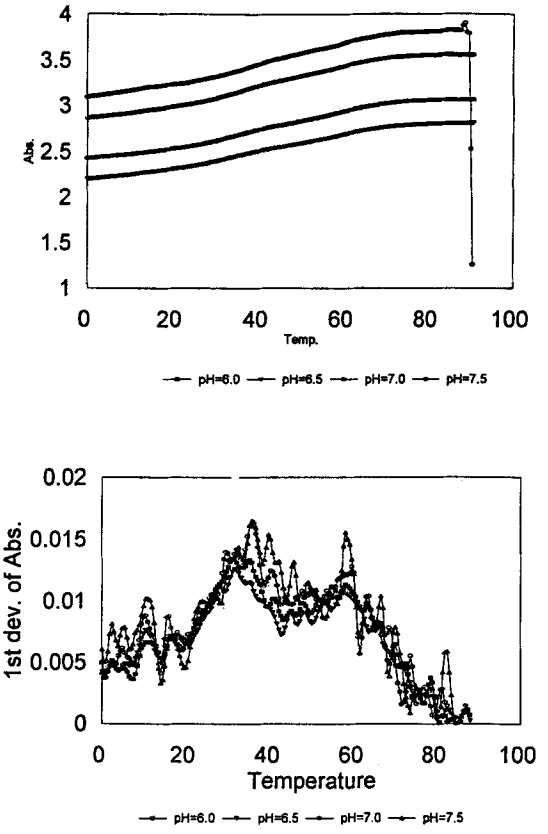

FIGURE VIII. The antiparallel pyrimidine motif **5** displayed an identical result in all pH range.

geometry fitness and matching base pairs. That the T_m of **4** (68 °C) is higher than the double helical denaturalization T_m of **5** (56 °C) can be explained by the fact that the parallel T:A:T triplex **4** has nondistinguishable stack energy among the individual strands. On the other hand, the first derivatives of T_m for less fitted triple helical antiparallel T:A:T sequence **5** gave two Gaussian line type maxima. The higher temperature peak corresponds to the T_m of the double helix, and the lower temperature peak corresponds to the T_m of the third strand. Thus, the triple helix of **5** is composed of a normal double helix (high T_m) and a weaker third strand (lower T_m). This denaturalization of two melting temperature patterns indicates that the triplex in this case may not fit tight enough together to form a homogenous triplex as sequence **5**. In general, we could summarize that the

profile of symmetry and steepness of the double and triple helical melting curves, after the first derivative analyses, can optimally be used to estimate the stability and mismatching of tested helical structural forms. The more symmetrical shape, higher and steeper peak represents the more stable and less mismatched base pairs in the test sequences. Sequence **6** is a mixture of two different classes of triplexes, *i.e.*, pyr:pur:pyr and pyr:pur:pur (1:3). It does not surprise us that they only gave a very weak interaction between the double helix and the mismatched third strand. This weak interaction was evident by their slow climbing curve before melting temperature (78 °C) in the first derivative temperature *vs.* absorbance relationship. The C:G:C combination base pairs needed protonation on cytidine residue to build up the Hoogsteen hydrogen bonding for triple helix base recognition. In our study, the antiparallel sequence **7** gave a typical example of C:G:C (Cs in the third strand are 5-MeCdR). The triplex had a stronger stability in pH = 6.00 NaCl than in pH greater than 6.0.

Our study has shown that with the right interactions between the third strand and the double helix, an excellent triple helix formation can be achieved.

REFERENCES

1. Rosenberg, I.; Farras Soler, J.; Tocik, Z.; Ren, W-Y.; Ciszewski, L. A.; Kois, P.; Pankiewicz, K. W.; Spassova, M. K.; Watanabe, K. A. *Nucleosides Nucleotides* **1993**, *12*, 381.
2. Kois, P.; Tocik, Z.; Ren, W-Y.; Spassova, M. K.; Rosenberg, I.; Farras Soler, J.; Watanabe, K. A. *Nucleosides Nucleotides* **1993**, *12*, 1093.
3. Kois, P.; Watanabe, K. A. *Coll. Czech. Chem. Commun.* **1993**, *58* (Special Issue), 167.
4. Kois, P.; Watanabe, K. A. *Nucleic Acid Res. Symp Ser.* **1993**, *29*, 215.
5. Ren, W-Y.; Watanabe, K. A. 207Th ACS National Meeting, March 13-17, 1994, San Diego, Abstr. # CARB 0068.
6. Felsenfeld, G.; Davies, D. R.; Rich, A. *J. Am. Chem. Soc.* **1957**, *79*, 2023.
7. Michelson, A. M.; Massoulie, J.; Guschlbauer, W. *Prog. Nucleic Acid Res. Mol. Biol.* **1967**, *6*, 83.
8. Broitman, S. L.; Im, D. D.; Fresco, J. R. *Proc. Nat. Acad. Sci. USA* **1987**, *84*, 5120.
9. Letai, A. G.; Palladino, M. A.; Fromm, E.; Rizzo, V.; Fresco, J. R. *Biochemistry* **1988**, *27*, 9108.
10. Arnott, S. A.; Bond, P. J.; Selsing, E.; Smith, P. J. C. *Nucleic Acid Res.* **1976**, *3*, 2459.
11. Moser, H. E.; Cervan, P. B. *Science* **1987**, *238*, 645.
12. Cooney, M.; Czernuszewicz, G.; Postel, E. H.; Flint, S. J.; Hogan, M. E. *Science* **1991**, *241*, 456,
13. Beal, P. A.; Dervan, P. B. *Science* **1991**, *251*, 1360.
14. Pilch, D. S.; Levenson, C.; Shafer, R. H. *Biochemistry* **1991**, *30*, 6081.
15. Durland, R. H.; Kessler, D. J.; Gunnell, S.; Duvic, M.; Pettitt, B. M.; Hogan, M. E. *Biochemistry* **1991**, *30*, 9246.
16. Watanabe, K. A.; Reichman, U.; Hirota, K.; Lopez, C.; Fox, J. J. *J. Med. Chem.* **1979**, *22*, 21.

17. Trousdale, M. D.; Nesburn, A. B.; Su, T-L.; Watanabe, K. A.; Fox, J. J.; Philips, F. S. *Cancer Res.* **1983**, *23*, 808.
18. Fourel, I.; Hantz, O.; Watanabe, K. A. Jacquet, C.; Chomel, B.; Fox, J. J.; Trepo, C. *Antimicrob. Agents Chemother.* **1990**, *34*, 473.
19. Burchenal, J. H.; Chou, T-C.; Lokys, L.; Smith, R. S.; Watanabe, K. A.; Su, T-L.; Fox, J. J. *Cancer Res.* **1982**, *42*, 2598.
20. Chou, T-C.; Burchenal, J. H.; Schmid, F. A.; Braun, T.J.; Su, T-L.; Watanabe, K. A.; Fox, J. J.; Philips, F. S. *Cancer Res.* **1982**, *42*, 3957.
21. Howard, F. B.; Frazier, J.; Lipsett, M. N.; Miles, H. T. *Biochem. Biophys. Res. Commun.* **1964**, *17*, 93.
22. Dervan, P. B. *Science* **1986**, *232*, 464.
23. Sklenar, V.; Feigon, J. *Nature* **1990**, *345*, 936.
24. Matteucci, M. D.; Caruthers, M. H. *J. Am. Chem. Soc.* **1981**, *103*, 3185.
25. Beaucage, S. L.; Caruthers, M. H. *Tetrahedron Lett.* **1981**, *22*, 1859.
26. McBride, L. J. Caruthers, M. H. *Tetrahedron Lett.* **1983**, *24*, 245.
27. Fox, J. J.; Van Praag, D.; Wempen, I.; Doerr, I. L.; Cheong, L.; Knoll, J.; E.; Eidinoff, M. L.; Bendich, A.; Brown, G. B. *J. Am. Chem. Soc.* **1959**, *81*, 178.
28. The collected data were transferred to a PC computer *via* a RS232 port. The ACSII file was saved as DOS format for later studies. The spreadsheet program we used for this analysis was Quattro Pro 5.0 for the Windows version. The data were imported into a spreadsheet as a comma and delimited file. This process is essential at this time otherwise the program will label the data as a character and not numeric any more. Most transferred utilities only recorded the dependent variables, although it was necessary to use the Block\|Fill tool of spreadsheet program to build the temperature step column for operation and the Block\|Sort tool to rearrange the temperature reading and absorbance in the same order. The regular temperature *vs.* absorbance curves can be plotted directly. It was easier to adjust the baseline and overlay the different spectra in one chart for better representation than to read the direct print out from the spectrophotometer. In order to solve the spreadsheet calculations and to analyze for our data sets, we developed our own programs in terms of macros to overcome data calculation problems.
29. The macro \h is a simple program to process two tasks: A, to sum five data points and divide by five to give the average value and B, to automatically move down five cells to start a new loop. We also inserted an "if" statement to stop at the end of the column.
\h is very useful macro to give avg each 5 data points on the right side of calculated column
{left}
{if @cellpointer("type")<>"v"}{quit}
{right}
{putcell "@sum(C(-1)R(0)..C(-1)R(5))/6"}{BlockValues C(0)R(0),C(0)R(0)}
{down 5}
{Branch \h}
30 This changed the 0.1 step temperature measure to 0.5 step. Each time the macro \b moved down one cell and tested the remainder of cell value, which multiplied by ten and divided by integer five. If it did not equal to zero, then it deleted the cell and the neighboring cells in the same row.
\b will delete limit rows in the column if it is empty.
{Left}
{if @cellpointer("type")<>"v"}{BlockDelete.Rows c(2)r(0)..c(0)r(0),partial}{up}
{down}{branch \b}
31. The macro \a was the major operator for calculation. \a will serve as the major tool for the 1st derivative.
{Regression.Independent C(-3)R(0)..C(-2)R(5)}
{Regression.Dependent C(-2)R(0)..C(-2)R(5)}

{Regression.Output C(0)R(0)}
{Regression.Y_intercept compute}
{Regression.Go}
{left 2}{down}{putcell"+$c(4)$r(6)*c(-1)r(0)+$c(5)$r(0)"}{right 2}{up}
{BlockCopy C(2)R(7),C(-1)R(0)}
{down}{left 2}
{if @cellpointer("type")<>"v"}{quit}
{right 2}{branch \a}

32. Blackburn, G. M.; Gait, M. J. Nucleic Acids in Chemistry and Biology, Oxford University Press, 1990, p. 58.

33. Raghunathan, G.; Miles, H. T.; Sasisekharan, V. Biochemistry 1993, 32, 455.